World Scientific
www.worldscientific.com

JAPAN SOCIETY OF CIVIL ENGINEERS
COASTAL ENGINEERING COMMITTEE

Coastal Engineering Journal, Vol. 53, No. 3 (2011) 223–243

DOI: 10.1142/S0578563411002343

ENSEMBLE EMPIRICAL MODE DECOMPOSITION ON STORM SURGE SEPARATION FROM SEA LEVEL DATA

LI-CHUNG WU

Coastal Ocean Monitoring Center, National Cheng Kung University, No. 1, University Rd., Tainan 701, Taiwan, R.O.C.

CHIA CHUEN KAO, TAI-WEN HSU* and KUO-CHING JAO

Department of Hydraulic and Ocean Engineering, National Cheng Kung University, No. 1, University Rd., Tainan 701, Taiwan, R.O.C.
**twhsu@mail.ncku.edu.tw*

YI-FUNG WANG

Water Resources Agency, Ministry of Economic Affairs, 9-12F, No. 141-3, Sec. 3, Hsin-Yi Rd., Taipei 106, Taiwan, R.O.C.

Received 22 July 2010
Revised 5 April 2011

This paper concerns the storm surge calculation based on the algorithm of ensemble empirical mode decomposition (EEMD). An accurate storm surge result is key information for coastal disaster warning and prevention. Separation of storm surge magnitude from sea level data has typically been done by specifying tidal input from main tidal harmonics. Obtaining accurate storm surge magnitude with harmonic analysis (HA) requires at least one month. This study discusses possible storm surge separation from short-term sea level time series using EEMD. The current work reveals that EEMD is predominant for short-term sea level data analysis shorter than thirty-five days. Due to different residues obtained from EEMD, this work proposes a method to determine most ideal residue for representing the storm surge.

Keywords: Ensemble empirical mode decomposition; harmonic analysis; storm surge; sea level data.

*Corresponding author.

1. Introduction

The coastal region is a sensitive area within the boundaries of air, sea and land, and suffers the impacts from these environments. Severe disasters, such as flooding, may occur due to extreme meteorological and oceanic impacts upon coastal area topography. To ensure coastal safety, a number of complex factors need to be considered. The storm surge is one of the relevant factors facing most coasts worldwide; a highly complex factor in coastal behavior. Due to obvious low-pressure, coastal water levels increase under storm conditions. In addition, water volume is pushed towards the shore by swirling winds. This rise in sea level can cause severe flooding in coastal areas, particularly when the storm surge coincides with normal high tides. In areas with large tidal ranges, storm surge can be most damaging while in the presence of high tide. In addition to coastal flooding, storm-driven waves reach the front of dunes due to the rising sea level, possibly resulting in near-shore erosion [Silvester and Hsu, 1997].

Storm surge features are quite complex The interaction between storm system and land also alter surge characteristics. To effectively understand the features of storm surge, some studies used statistical approaches to analyze changes in the occurrence and severity of storm surge events [Butler *et al.*, 2007; Vrijling, 2001]. To describe the statistical features of storm surges, adequate surge data samples are necessary. Numerical models are also common tools to obtain the surge information [Eric and Marshall, 2009]. Earlier researches show that surface winds must be specified as a function of both space and time [Bode and Hardy, 1997; Moon *et al.*, 2009]. Observations of meteorological data in the coasts are not always complete, thus limiting surge calculation. *In situ* sea level measurement plays an important role in evaluating and describing surge characteristics. Separating storm surge magnitude from sea level data has typically been done by specifying tidal input from main tidal harmonics. Due to regular astronomical processes, we can regard oceanic tides as inherently regular. Harmonic analysis (HA) often describes water level variation as the sum of a constant mean level, continuous from specific harmonics and a residual. The residual from sea level data by HA can be seen as all nontidal effects on the sea level. The positive and negative residuals are induced by wind stress, pressure depression and wave set-up during typhoon events. On the right side of the typhoon the positive residual surges are observed, while on the left side of the typhoon the negative surges occur along the coast. Also, the sea level rise is associated with the wave effect along the open coast due to the radiation stress [Kim *et al.*, 2010]. However, separating these from the nontidal residual is difficult. Because storm surge is the dominant phenomenon inducing sea level rise during typhoons, some studies consider the nontidal residual as the storm surge [Lee, 2006; De Oliviera *et al.*, 2009]. This study also treats the nontidal residual as the storm surge instead of discussing how to separate the storm surge, wave run-up, tsunamis, and climatic effects.

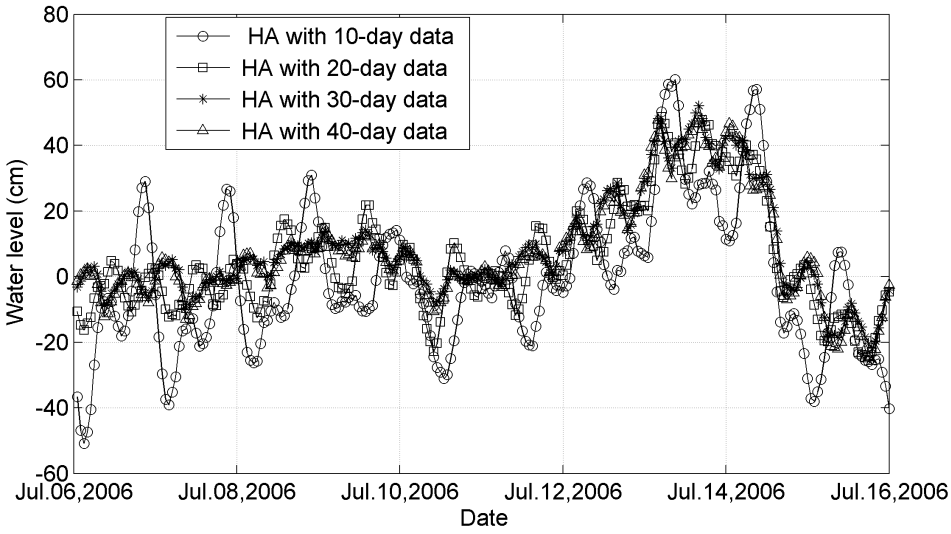

Fig. 1. Nontidal residuals calculated by HA with different lengths of sea level records.

HA is an ideal method to separate tide components and storm surge from sea level record. To obtain storm surge magnitude accurately, we need enough length of sea level record to determine the tidal harmonic components. Obtaining accurate storm surge magnitude by HA requires at least one month sea level data, and reliable calculation accuracy by HA increases with the length of sea level record [Reeve *et al.*, 2004]. Figure 1 shows different lengths of *in situ* sea level data analyzed by HA to calculate the nontidal residual. Periodic oscillations for data lengths less than thirty days are quite obvious. This means that the periodic components and nonperiodic residual cannot be separated effectively by HA under this situation. As a result, this study cannot obtain accurate storm surge data by HA for short-term sea level data. In case the data is not long enough to obtain surge magnitude by HA, other applicable methods are needed to address this subject.

Huang *et al.* [1998] proposed the algorithm of empirical mode decomposition (EMD) for nonlinear and nonstationary data processing [Nunes *et al.*, 2003]. The decomposition is based on the local characteristic time scale of the signal and it is applicable to nonstationary processes [Zhang and Gai, 2006]. Due to the problem of mode mixing for determining correct components, Wu and Huang [2008] improved the algorithm, naming it EEMD which has proved to be versatile in a broad range of applications for nonlinear and nonstationary data processes [Gan *et al.*, 2008; Peel *et al.*, 2009]. Unlike the HA which decomposes the analyzed data as different sine/cosine components, the EEMD decomposes the signal as different intrinsic mode functions (IMFs) as defined by Huang *et al.* [1998]. In addition to IMFs, residues separated from sea level data also provide significant information. Ho *et al.* [2004] retrieved sea surface temperature trends to discuss warming trends of different seasons. McMahon *et al.* [2007] analyzed global streamflows, revealing that

the intra-decadal streamflow component significantly relates to the residual or trend component. Based on previous studies, the EEMD should be workable to extract storm surge magnitude from the sea level record. It is the purpose of this article to develop a procedure for deriving storm surge magnitude from residuals of short-term sea level time series by implementing the EEMD. To verify the practicability of this work, the current study proposes a theoretical basis for deriving surge. Sea level data from different cases are used to discuss the accuracies and the features of the surge results Finally, we verify the predominance of EEMD for short-term sea level data analysis.

2. Theoretical Preliminaries

Introducing the EEMD algorithm begins from the EMD. The EMD technique is capable of decomposing time series into different oscillating intrinsic components which are called IMFs. Depending on the nature of the time series under study, the IMFs and the residual component may exhibit linear or nonlinear behavior [McMahon *et al.*, 2007]. Unlike the Fourier transform, an IMF is not restricted to a narrow band signal, but can be both amplitude and frequency modulated. Based on the idea of Huang *et al.* [1998], the time series of sea level $x(t)$ can be decomposed by the EMD as follows:

(i) Identify all the maxima and minima of $x(t)$ within the whole time domain.
(ii) After identifying the extrema of $x(t)$, all the local maxima are connected by a cubic spline as the upper envelope $U(t)$. Problems of the spline fitting may occur near the ends, where the cubic spline fitting can have large swings. Even with these problems, Huang *et al.* [1998] pointed out that the sifting process can still extract the essential scales from the data. Repeat the similar procedure for the local minima to produce the lower envelope $L(t)$. $U(t)$ and $L(t)$ should cover $x(t)$ between them.
(iii) Compute the average of upper and lower envelopes, $m(t) = [U(t) + L(t)]/2$.
(iv) Subtract $m(t)$ from $x(t)$ to extract the detail, $h(t) = x(t) - m(t)$. $h(t)$ may be the first IMF from the time series.
(v) Check whether $h(t)$ is an IMF or not.

Ideally, $h(t)$ should be an IMF. However, overshoot and undershoots of the data processing are common, which can also generate new extrema, and shift or exaggerate the existing ones. Each IMF should meet the following requirements. First, the local maxima of the data series are always positive and the local minima are negative, respectively [Daetig and Schlurmann, 2004]. In other words, the number of extrema and the number of zero crossings must either equal or differ at most by one. Second, the mean value of the envelopes defined by the local maxima and by the local minima is zero at any data location. This idea modifies the classical global requirement to a local one so that the instantaneous frequency will not have unwanted fluctuations induced

by asymmetric wave forms. Ideally, the requirement should be a zero local mean. Huang *et al.* [1998] pointed out that the envelope mean $m(t)$ may be different from the true local mean for nonlinear data; consequently, some asymmetric wave forms can still exist no matter how many times the data are sifted. If $h(t)$ satisfies the requirements above, then extract IMF and replace $x(t)$ with the first residual $r(t)$:

$$r(t) = x(t) - h(t)\,. \tag{1}$$

If $h(t)$ is not an IMF, then further sifting is necessary, to replace $x(t)$ with $h(t)$

(vi) Repeat steps (i)–(v) until no more IMF can be extracted and the residual, r_n, becomes a monotonic function from which no more IMFs can be extracted. The whole EMD procedure can be described as the flow chart of Fig. 2 Wu and Huang [2008] pointed out that the EMD data composition may consist of different physical processes, or mode mixing, represented in an IMF, caused mostly by intermittent driving mechanisms. Mode mixing is defined as any IMF consisting of oscillations of dramatically disparate scales. Any IMF which

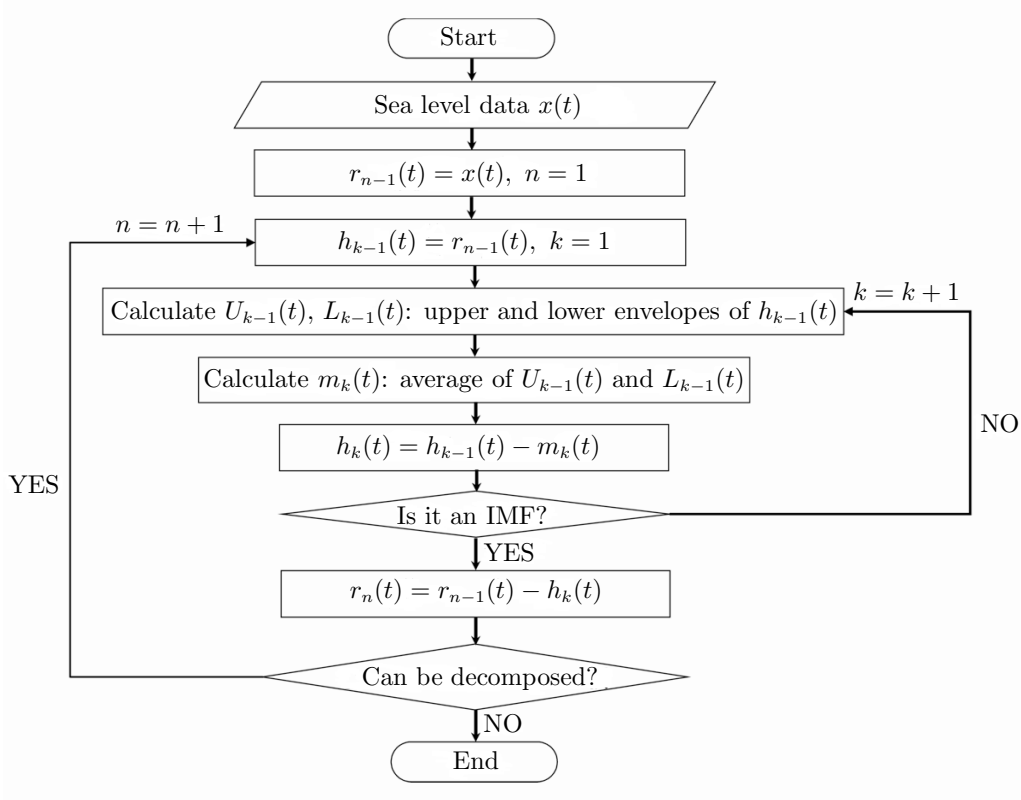

Fig. 2. EMD flow chart for separating storm surge magnitude from sea level data $x(t)$. In the figure, $h_k(t)$ is IMF if $h_k(t)$ satisfy the requirements which we mentioned in the section of theoretical preliminaries. $r_n(t)$ is the residual after separating the IMF for sea level data.

occurs through mode mixing ceases to have physical meaning by itself and may result in wrong separation of storm surge from sea level data. To overcome the IMF mode mixing problem, Wu and Huang [2008] proposed the EEMD, in which added white noise populates the whole time–frequency domain with constituting components of different scales before starting the EMD process. This data preprocess is the main difference between EMD and EEMD. The added white noise plays the role of filling in different scales of the original signal where the noise can be cancelled out in the ensemble mean when enough trials are used in the EEMD process [Zhang *et al.*, 2009]. When signal is added to this white background, signal bits of different scales are automatically projected onto proper scales of reference established by the white noise in the background. Though EEMD adds different white noise to the data, the mean of IMFs of different cases in the later procedure efficiently reduces white noise influence. Theoretically, infinite number of ensemble trials would cancel out the added white noise completely. However, this is not feasible for real-world applications. Zhang *et al.* [2009] suggest that number of ensemble trials should be approaching 100. This value is adopted in this study. Figure 3 shows the whole EEMD procedure. We generate 100 different zero-mean Gaussian white noise series based on the normally distributed random numbers, and add different

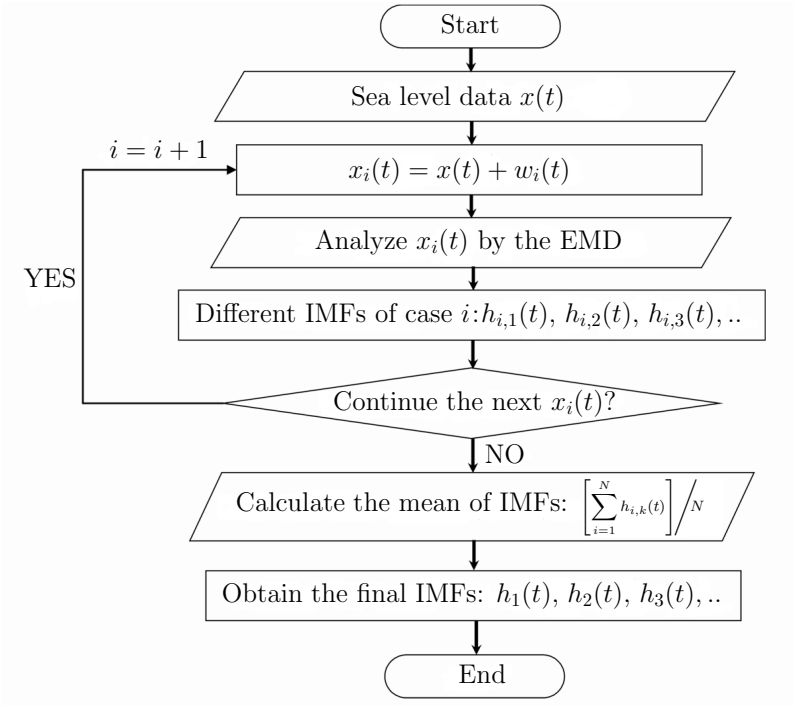

Fig. 3. EEMD flow chart for separating storm surge magnitude from sea level data $x(t)$. In the figure, $w_i(t)$ is white noise.

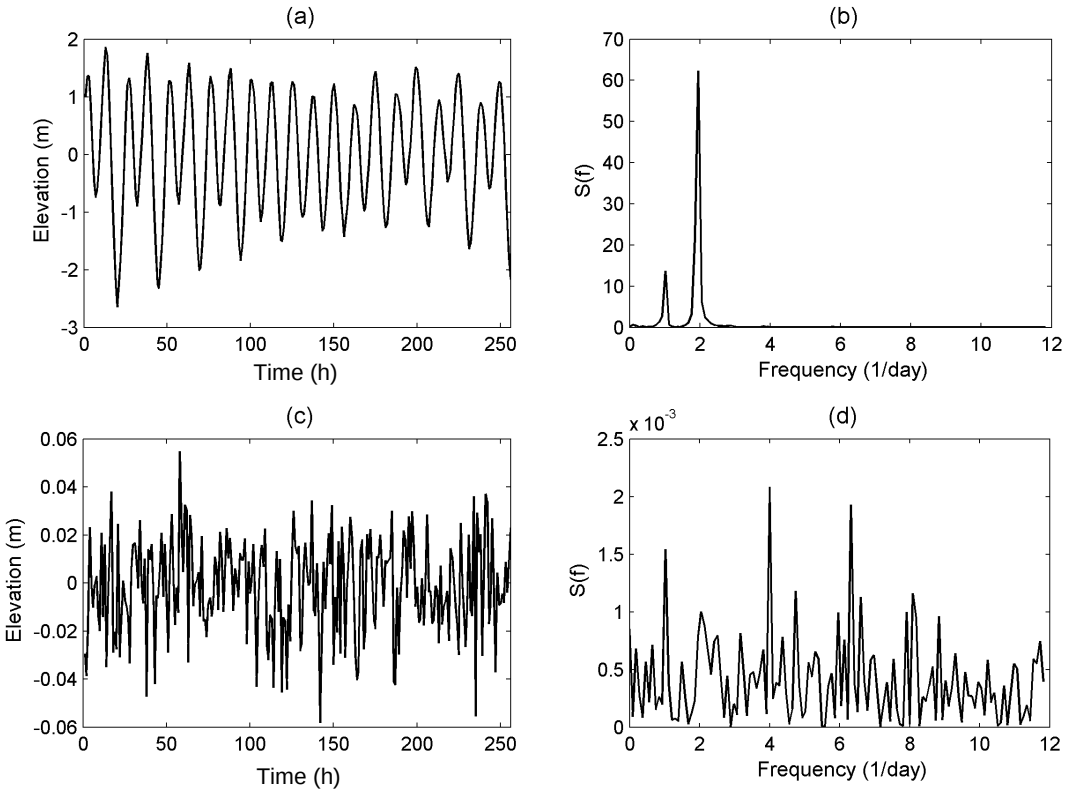

Fig. 4. (a) *In situ* sea level time series; (b) energy spectrum of sea level time series; (c) the Gaussian white noise series; and (d) energy spectrum of white noise.

white noise series to the sea level series, respectively. By the EMD procedure of these noise-added sea level series, we can obtain 100 different IMFs: $h_{i,1}(t)$, $h_{i,2}(t), \ldots,$ where $i = 1, 2, \ldots, 100$. Average these 100 IMFs, respectively, we can obtain the final IMFs: $h_1(t)$, $h_2(t), \ldots$. Figure 4 shows the cases of sea level data and the created white noise. Figures 4(a) and 4(b) represent one case of *in situ* sea level data and its energy spectrum where the energy density focuses around 1 day^{-1} and 2 day^{-1}. Figures 4(c) and 4(d) represent one case of the zero-mean Gaussian white noise series and its energy spectrum. The white noise spectrum shows that the energy is distributed within the whole frequency domain. The sampling rate of our sea level data is 24 day^{-1}. Based on the Nyquist frequency, the white noise in the frequency domain is within domain of $(0, 12)$ day^{-1}.

3. Sea Level Data Analysis by EEMD

3.1. *Data collection*

Sea level records used here are measured at nine different tide stations around Taiwan (Fig. 5). Taiwan locates between the tropics and the subtropics, averaging

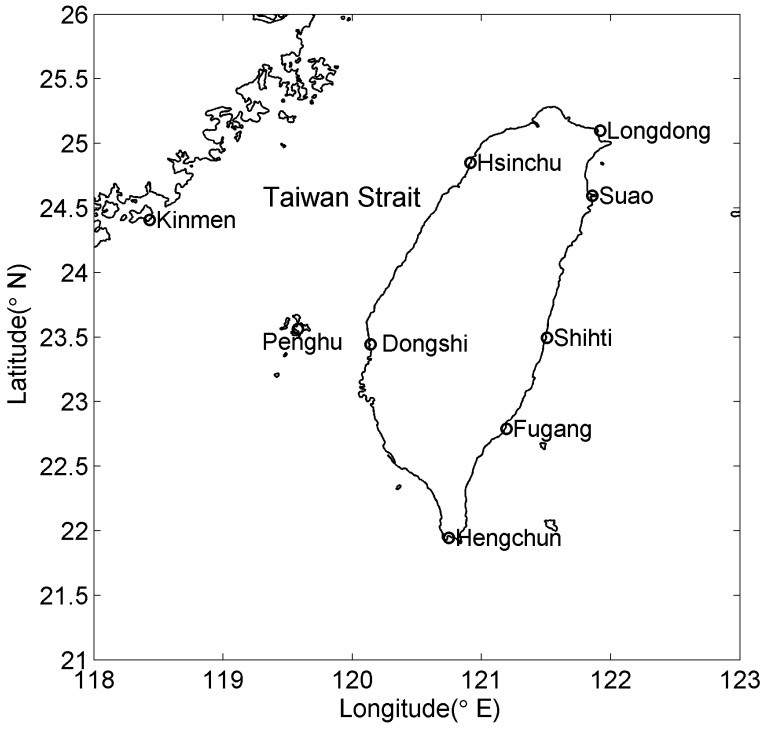

Fig. 5. Tide stations whose data are used in this study.

3.5 typhoons attacks every year. Surge characteristics on the Western and Eastern side of Taiwan are quite different. The current work collects sea level records from 2001–2007 at nine different tide stations. This research applies the *in situ* sea level records to verify EMD practicability to derive storm surge magnitude from the short-term data. In addition to *in situ* sea level data, the worldwide tidal component data from satellites also provide powerful water elevation information offshore. The recorded time length of tidal data should not be a serious problem in theory. However, the tidal waves would be influenced by the near-shore topography. To obtain real tidal features within this area, coastal tide data are still necessary. Therefore, an applicable algorithm for short-term coastal tide data analysis is still significant.

3.2. *EEMD data analysis*

Figures 6 and 7 show the ten-day sea level records and its IMF results. Data input presents the original sea level data measured at the Shihti tide station on the Eastern side of Taiwan. Figure 6 shows that the IMF1 and IMF2 present components that oscillate about one to two times daily. These are mixed tides related to tides between the diurnal and semi-diurnal tides. However, the IMF1 and IMF2 waveforms are not monotonous sinusoidal waves and IMF frequencies and amplitudes are not steady. In other words, the IMFs present nonstationary characteristics of the data.

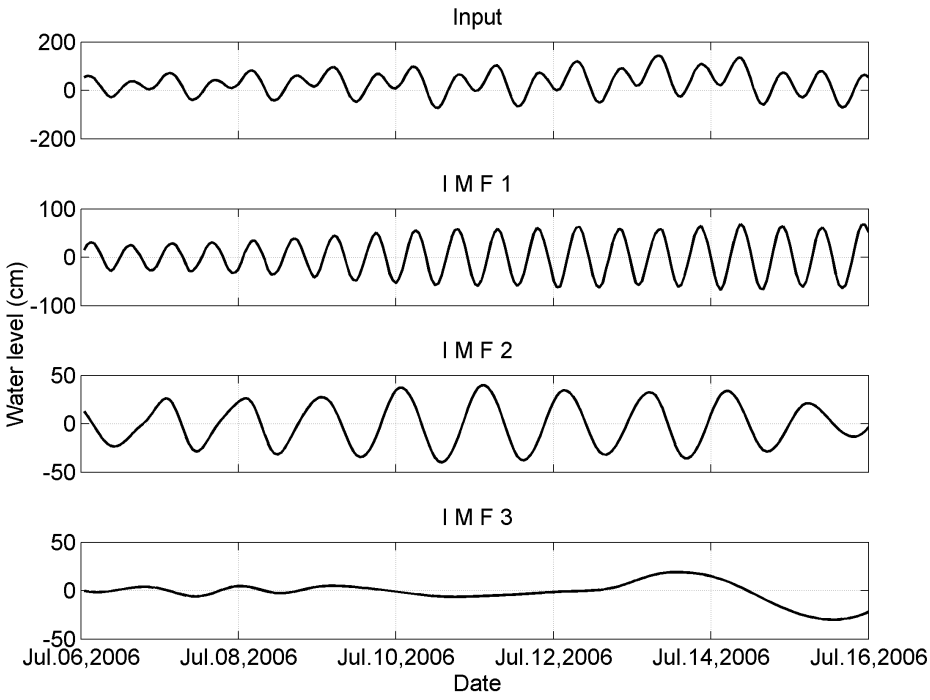

Fig. 6. Ten-day sea level records at the Shihti tide station and its IMFs.

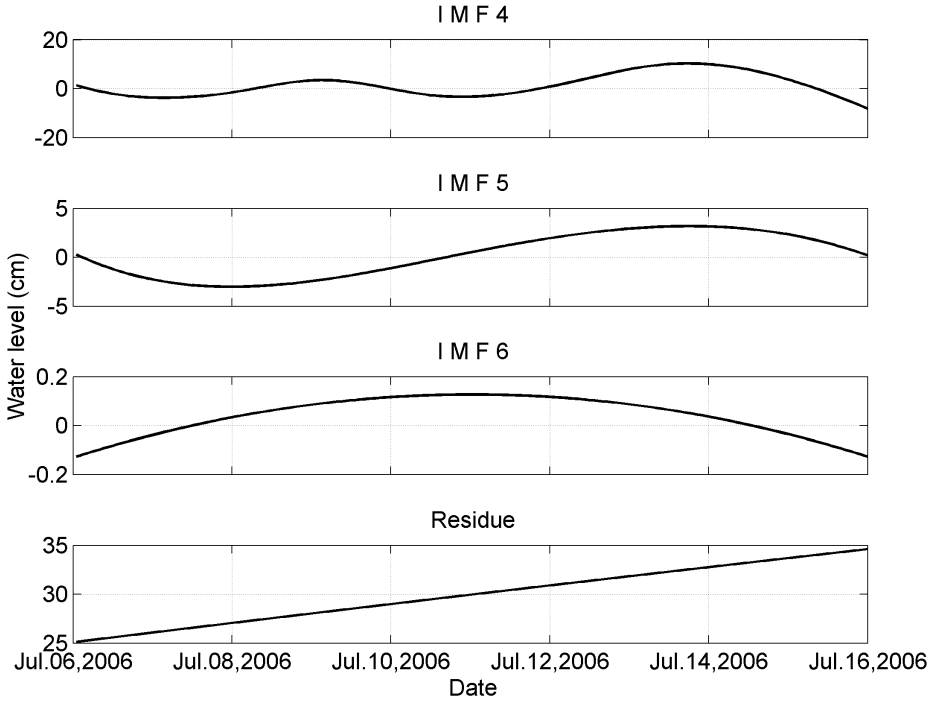

Fig. 7. Other IMFs and residue analyzed at the Shihti tide station.

To verify their frequency band, this study calculates the energy spectrum of different IMFs by the Fourier transform (FT) (Figs. 8 and 9). The peak frequencies of IMF1 and IMF2 are 1/12.2 h^{-1} and 1/25.6 h^{-1}. They are almost the same as frequencies of well-known diurnal and semi-diurnal tides. Based on Eqs. (2) and (3), different residues can be calculated by subtracting different IMFs from the sea level records:

$$r_1(t) = x(t) - h_1(t)\,, \tag{2}$$

$$r_{n+1}(t) = r_n(t) - h_{n+1}(t) \quad n \geq 1\,, \tag{3}$$

where $h_n(t)$ is the nth IMF, $r_n(t)$ is the nth residue. This work compares different residues $r_n(t)$ in Fig. 10. The reliable storm surge values $S_L(t)$ are calculated by the HA with six-year *in situ* sea level data whose length should be sufficient to separate periodic tides from nontidal residue. This case presents that the trend of $r_2(t)$ is quite similar to $S_L(t)$. Despite obvious deviations between $r_2(t)$ and $S_L(t)$, the deviations are stable with time. Thus, this research effectively reduces surge calculation error by subtracting the mean of these differences. Compared to the EEMD result, the HA residue with ten-day data $S_T(t)$ still contains obvious periodic oscillations. Since these oscillations are unstable and irregular, the difference between the $S_T(t)$ and $S_L(t)$ cannot be improved effectively. To verify accuracies of the storm surge calculation by EEMD and HA, this work calculates the root mean square deviation (RMSD, R_D) between $S_L(t)$ and calculated storm surges:

$$R_D = \sqrt{\frac{\sum_{i=1}^{n} \left[S_L(t_i) - \hat{\eta}(t_i)\right]^2}{n}}\,, \tag{4}$$

where $\hat{\eta}(t_i)$ is the calculated storm surge by the EEMD and HA from ten-day sea level records, and n is the number of total data sets. This research collects forty-three data sets of sea level records from each tide station during typhoon events. To present all the results from these data sets, we use the box and whisker plots. From each box and whisker plot, the top and bottom of each box are the 25th and 75th percentiles of the samples, respectively. The line in the middle of each box is the sample median. The upper and lower whiskers present the highest and lowest results from the samples. Figure 11 shows that the left box and whisker plot of every station present the RMSD between $S_L(t)$ and the calculated storm surge by the EEMD; the right box and whisker plot present the RMSD calculation by the HA. For each typhoon case, the current study obtains one value of R_D. The box and whisker plot presents the median, highest, lowest, 25th and 75th percentiles of the R_D samples. In Fig. 11, the left box and whisker plot from every station shows lower R_D values than the right one. This means the storm surge calculated results by EEMD are more accurate under the case of ten-day sea level record calculation.

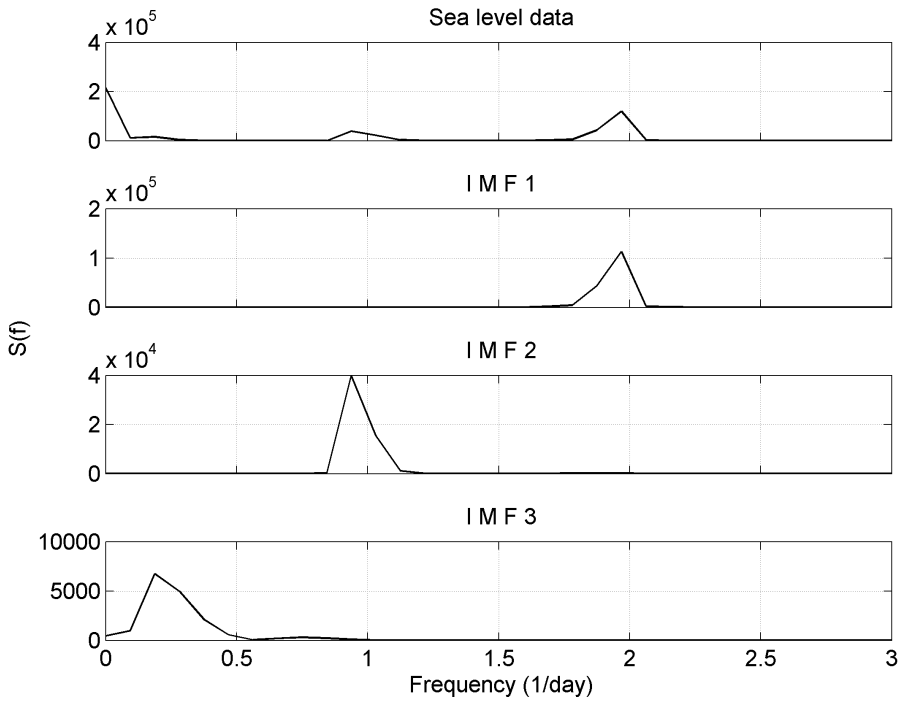

Fig. 8. The Fourier spectra of sea level records and its IMFs in Fig. 6.

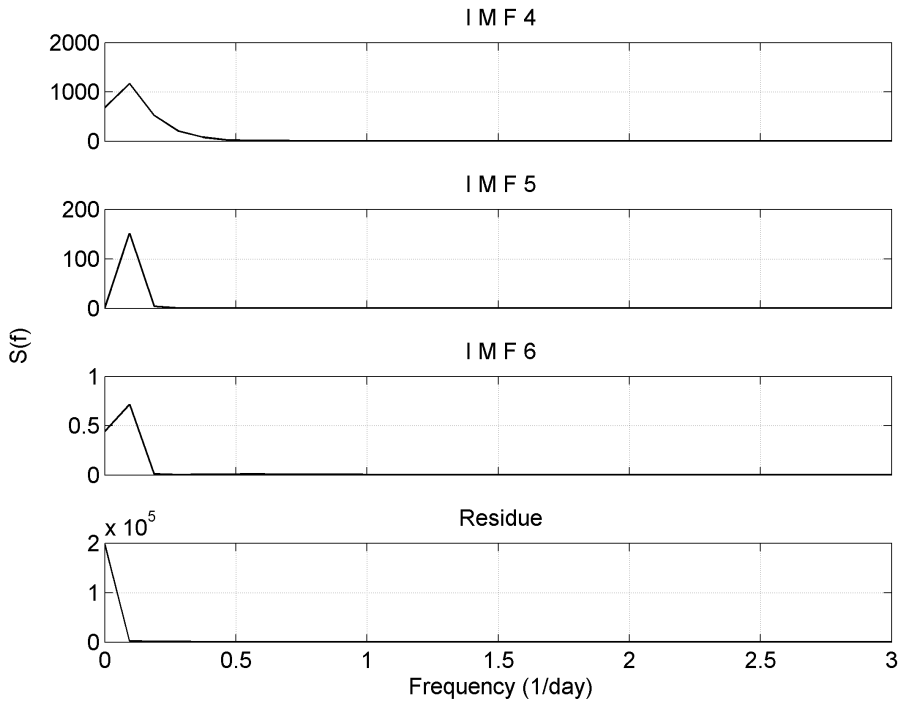

Fig. 9. The Fourier spectra of IMFs and residue in Fig. 7.

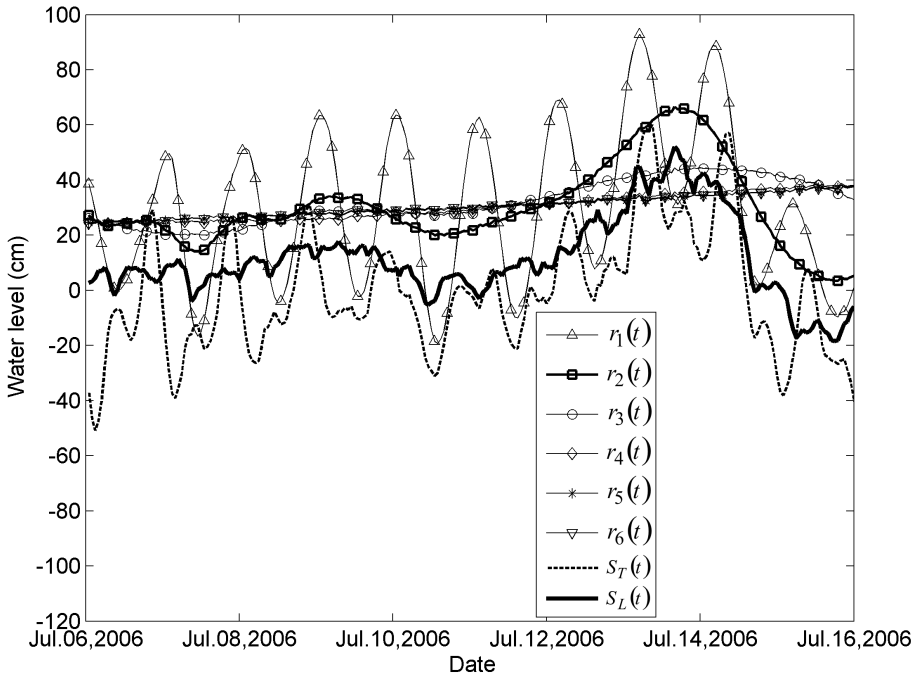

Fig. 10. The relationship among storm surge $S_L(t)$ and different residues analyzed at the Shihti tide station.

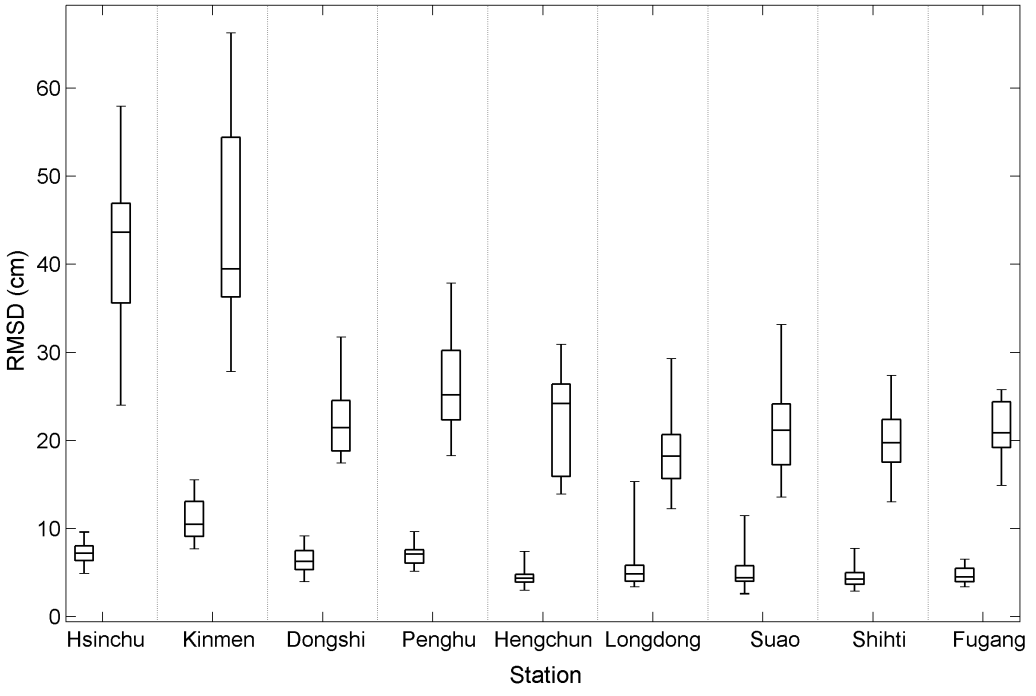

Fig. 11. The RMSD of storm surge calculation using EEMD (left box and whisker plots) and HA (right box and whisker plots).

4. Discussion

4.1. *Orthogonality and completeness of the IMFs*

These IMFs from EEMD helps in better understanding of the internal structure of the signal. The IMFs should be locally orthogonal to each other. The higher orthogonality corresponds to less leakage of information [Klionski *et al.*, 2008; Zhang and Gai, 2006]. To measure the efficiency of the IMFs, the orthogonality of the decomposition should also be checked. To check the orthogonality of the IMFs, Chang *et al.* [1997] and Molla *et al.* [2006] use the index of orthogonality (O_{jk}):

$$O_{jk} = \frac{1}{T} \sum_{t} \left\{ \frac{[h_j(t) \cdot h_k(t)]}{[h_j^2(t) + h_k^2(t)]} \right\} \quad j, k = 1 \sim (M+1)\,, \tag{5}$$

where h_j and h_k are jth and kth IMFs, $h_{M+1}(t)$ means the last residue after the EEMD. If the decomposition is orthogonal, then the value of O_{jk} should be zero [Zhang and Gai, 2006]. A set of perfect orthogonal IMF components will give zero values of O_{jk}. In practice, the accepted value O_{jk} is smaller than 0.1. As shown in Fig. 12, it presents the indices of orthogonality between all possible pairs of

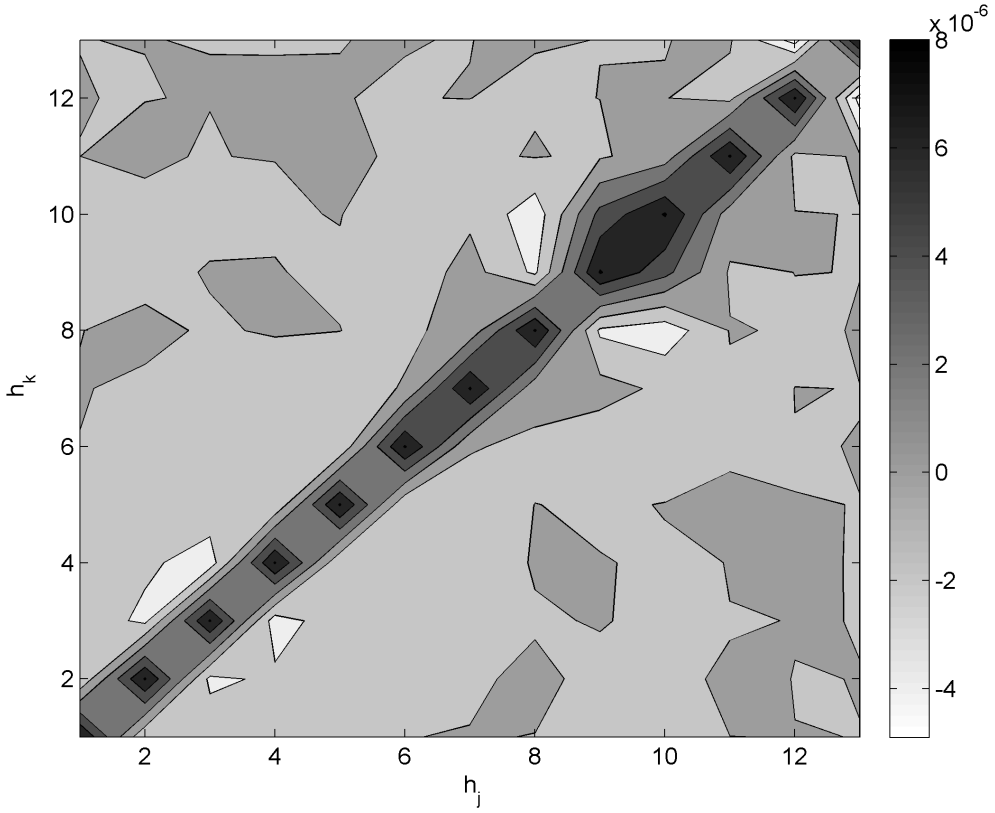

Fig. 12. The indices of orthogonality between all possible pairs of IMFs (Shiti station).

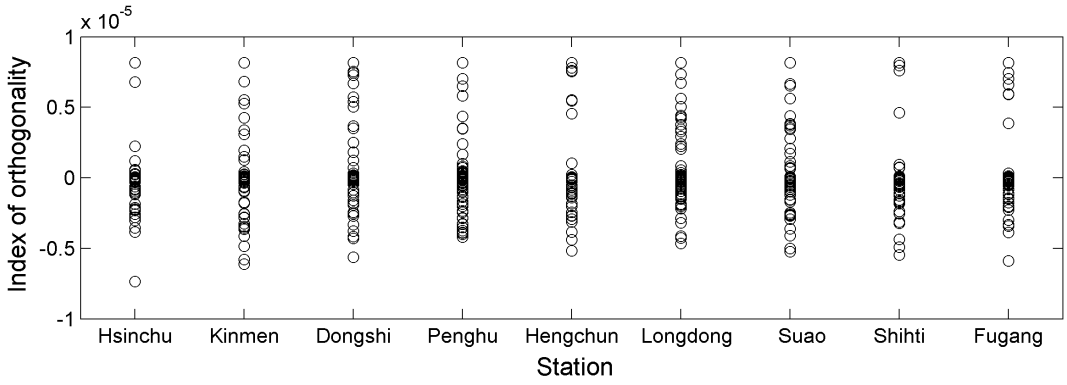

Fig. 13. The analyzed results of indices of orthogonality from the data set at different stations.

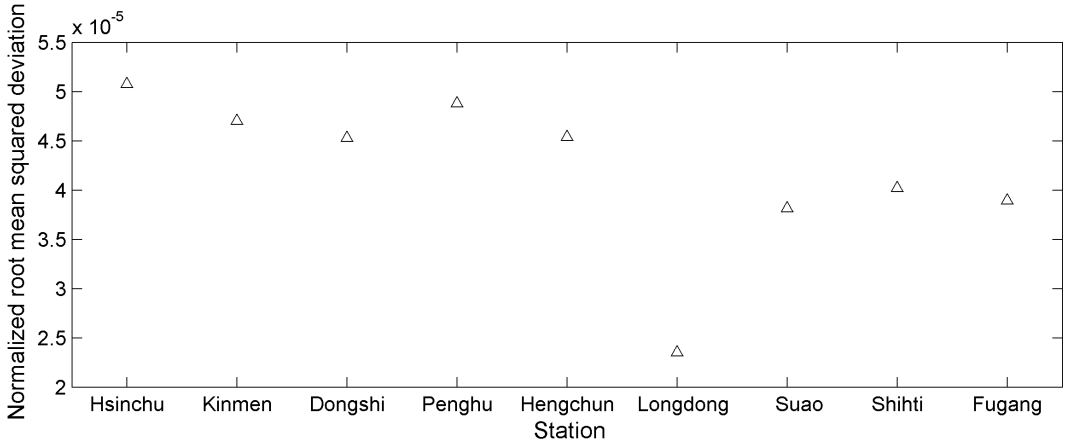

Fig. 14. The normalized root mean squared deviation between the original and reconstructed data.

IMFs from the data set in Shiti station. The IMFs are decomposed from the sea level data in Shiti station. The maximum value of the indices of orthogonality is of the order 10^{-5}. Figure 13 shows the indices of orthogonality from the data set in different stations around Taiwan. Each circle symbol in Fig. 13 presents the indices of orthogonality between h_j and h_k. It shows that all of the indices of orthogonality are substantially less 0.1. The orthogonality of sea level data is satisfied.

In addition to the orthogonality, the completeness of the EEMD on sea level data analysis should be identified too. To check the completeness, this study reconstructs the sea level data from all the IMF components. Figure 14 shows the normalized root mean squared deviation (NRMSD, R_N) between the original and reconstructed data

$$R_N = \frac{R_D}{(x_{\max} - x_{\min})}\,, \tag{6}$$

where $x_{\max}$ and $x_{\min}$ are the maximum and minimum of the sea level time series, respectively. Since different white noise is added to the time series, there are deviations between the original and reconstructed data. However, the mean of IMFs of different cases in the later procedure efficiently reduces deviations. The NRMSD is of the order 10^{-5} as shown in Fig. 14. It reveals that EEMD is a lossless decomposition for the sea level data and the completeness of the decomposition is thus demonstrated. By observing the orthogonality and completeness, this study reveals that the EEMD is applicable to decompose the sea level data.

4.2. *Accuracy of storm surge calculation by EEMD and HA*

Figure 11 presents that geographical locations of tide stations influence sea level data analysis by HA. The figure also presents poorer HA accuracies for tide stations located on the Western side of Taiwan, especially the middle part of the Taiwan Strait. This should be the reason for different tidal ranges. Figure 15 shows the analysis of maximum tidal ranges from forty-three typhoon events, revealing that tidal ranges on the Western Taiwan coasts are much higher than those in Eastern Taiwan. For the Kinmen station, all tidal ranges from different typhoon cases are larger than 4 m. As previously mentioned, HA cannot efficiently remove periodic components from short-term sea level data. As a result, tidal energy still partially attaches to the residue after HA. HA deviations should be obvious for high tidal range cases. Compared to HA results, EEMD calculated results show higher accuracy

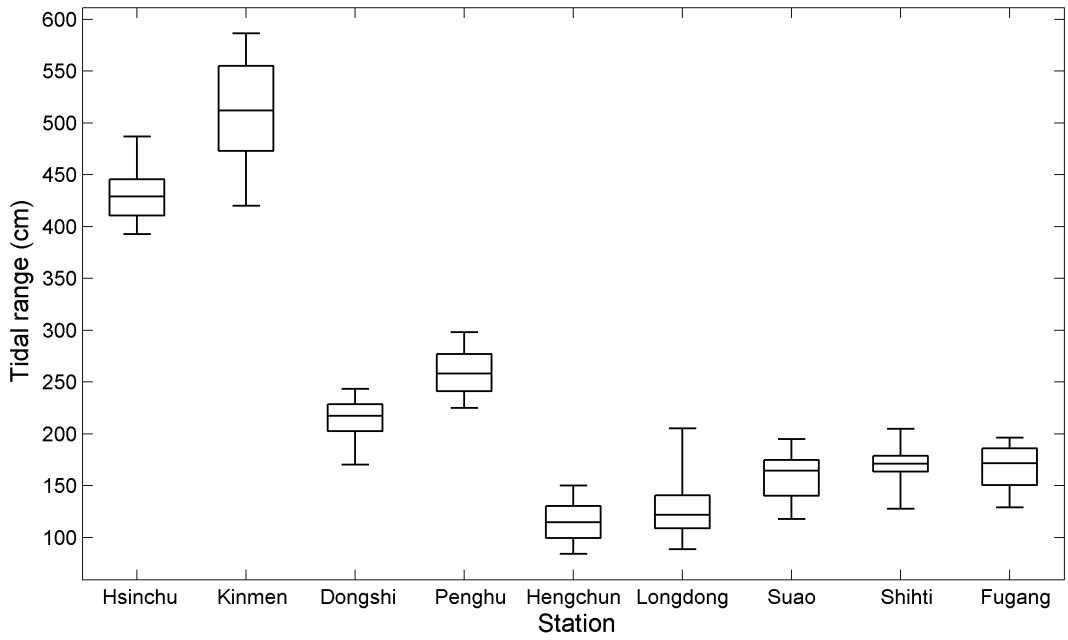

Fig. 15. Tidal range analyzed from different tide stations.

for short-term sea level data analysis. As presented by Huang *et al.* [1998], IMFs can be nonstationary components from the original data. This means that any IMF separated from sea level data by EEMD can be the time series with multi-periods and amplitudes. For short-term data analysis, long period tidal components over ten days can be combined together in the IMFs. This explains why Figs. 6 and 7 show IMFs as the nonstationary time series. As a result, EEMD residues can be separated from the periodic components more efficiently for short-term sea level data analysis.

Though the maximum RMSD by the EEMD can reach 15 cm as shown in Kinmen station of Fig. 11, it is much smaller than HA results for short-term data analysis. In addition, the calculated results by EEMD do not depend upon obvious tidal ranges. For high tidal range cases, synchronized high astronomical tide and storm surge are quite dangerous on the coasts. An accurate storm surge magnitude is key information for disaster warming and prevention. The EEMD shows the advantage of storm surge calculation for short-term analysis and high tidal range.

As mentioned, the EEMD is more advantageous than HA to analyze short-term sea level time series. To clarify storm surge calculation by EEMD and HA, this section discusses the relationship between the length of analyzed sea level data and the accuracy of storm surge calculation. Figure 16 shows that EEMD accuracy is stable with the length of analyzed data. Unlike EEMD results, HA accuracies

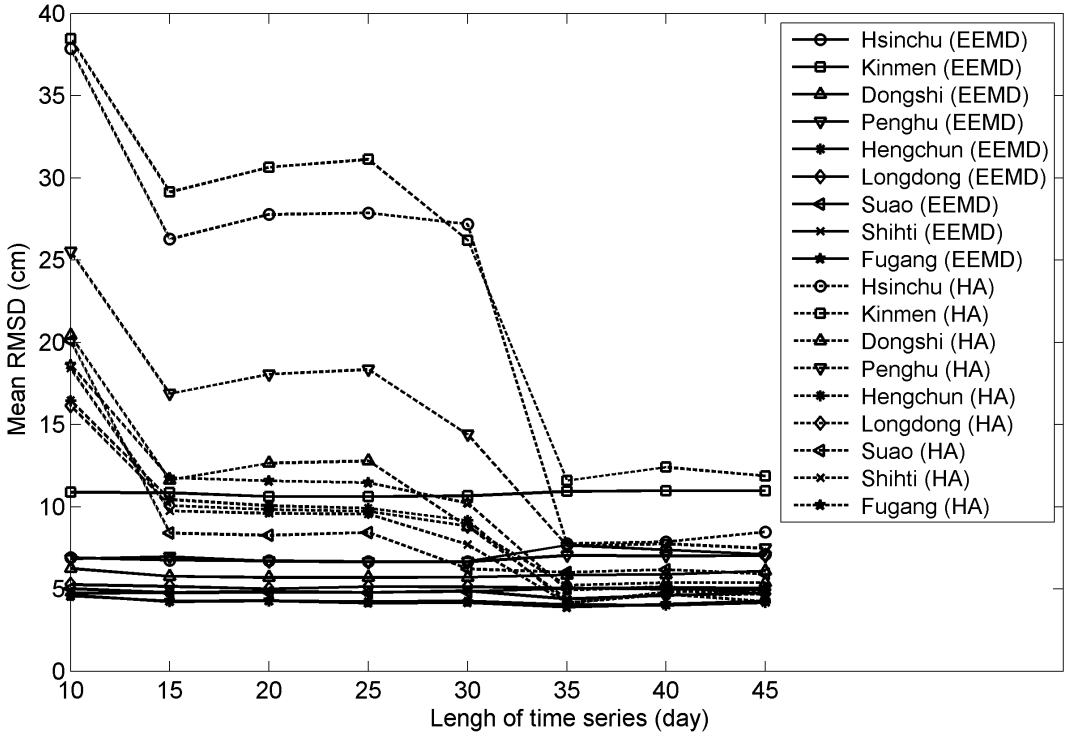

Fig. 16. Relationship between lengths of sea level time series and EEMD and HA accuracies.

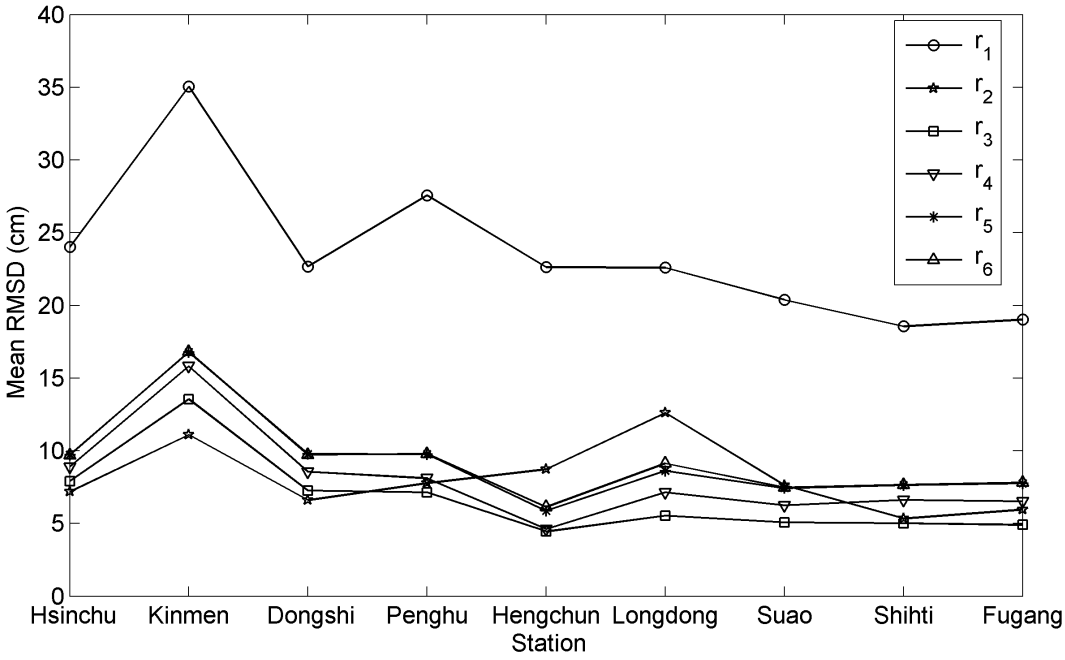

Fig. 17. Accuracy of different r_n representing storm surge.

improve with the longer length of analyzed data. For analyzed data longer than thirty-five days, the accuracies of HA and EEMD data analysis are similar. The results by HA should be accurate if sea level records are long enough. In other words, HA and EEMD should be complementary on storm surge calculation for data analysis of different lengths of sea level records. This work reveals that the EEMD is more predominant for short-term sea level data shorter than thirty-five days.

4.3. *The relationship between EEMD residue and storm surge*

Equations (2) and (3) show obtaining different IMFs and residues $r_n(t)$ by EEMD. The residues provide key information to describe the storm surge. This section discusses which residue provides accurate storm surge magnitude. The current study calculates deviations among the storm surge and different residuals. The mean RMSD of forty-three data sets from different typhoon cases are applied to determine accuracy of storm surge calculation. Figure 17 reveals that r_2 or r_3 more accurately describe storm surge than other residues except for the cases from Hengchun, Suao and Longdong. Equation (3) shows that the residue is calculated from IMF. We can discuss the residue characteristics from IMFs. Figure 18 shows calculating the Fourier spectra of IMF2. The spectra in the figure are averaged results, due to the analysis of forty-three data sets from different typhoon cases. Similar to the IMF2 spectral result in Fig. 8, all of the spectra in Fig. 18 present the energy density focus on the frequency band around 1 day^{-1}. Similar results occur from all other

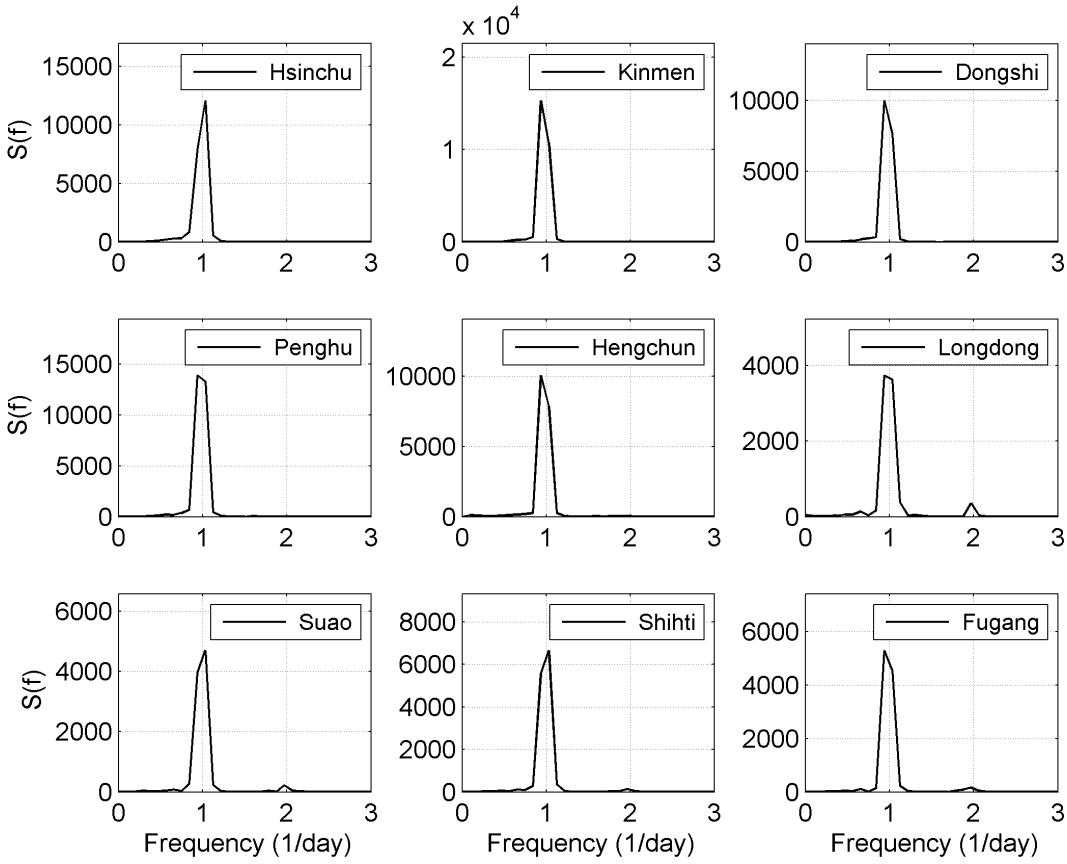

Fig. 18. Averaged spectra of IMF2 at different stations.

cases and they all approximate to the frequency band of diurnal tide. It seems the IMF2 should be capable of separating components approximate to the diurnal tide from our cases. However, the Fourier spectra of IMF3 (Fig. 19) shows that obvious energy approximate to the diurnal tide still attaches within the IMF3 in some cases. Figure 19 shows that the IMF3 spectra from Penghu, Hengchun, Longdong, Suao, Shihti, and Fugang maintain energy on the frequency band around 1 day^{-1}. In these stations, accuracy is poorer using r_2 to present the storm surge than using r_3. As discussed in the previous section, the r_2 and r_3 can be obtained by:

$$r_2(t) = x(t) - h_1(t) - h_2(t)\,, \tag{7}$$

$$r_3(t) = x(t) - h_1(t) - h_2(t) - h_3(t)\,, \tag{8}$$

where $h_n(t)$ is the nth IMF separated from the time series $x(t)$. The spectra show that some energy approximate to the diurnal tide still maintains within the $r_2(t)$. To accurately extract storm surge magnitude, it is more ideal to use $r_3(t)$ in which some diurnal tide energy have been removed from $r_2(t)$.

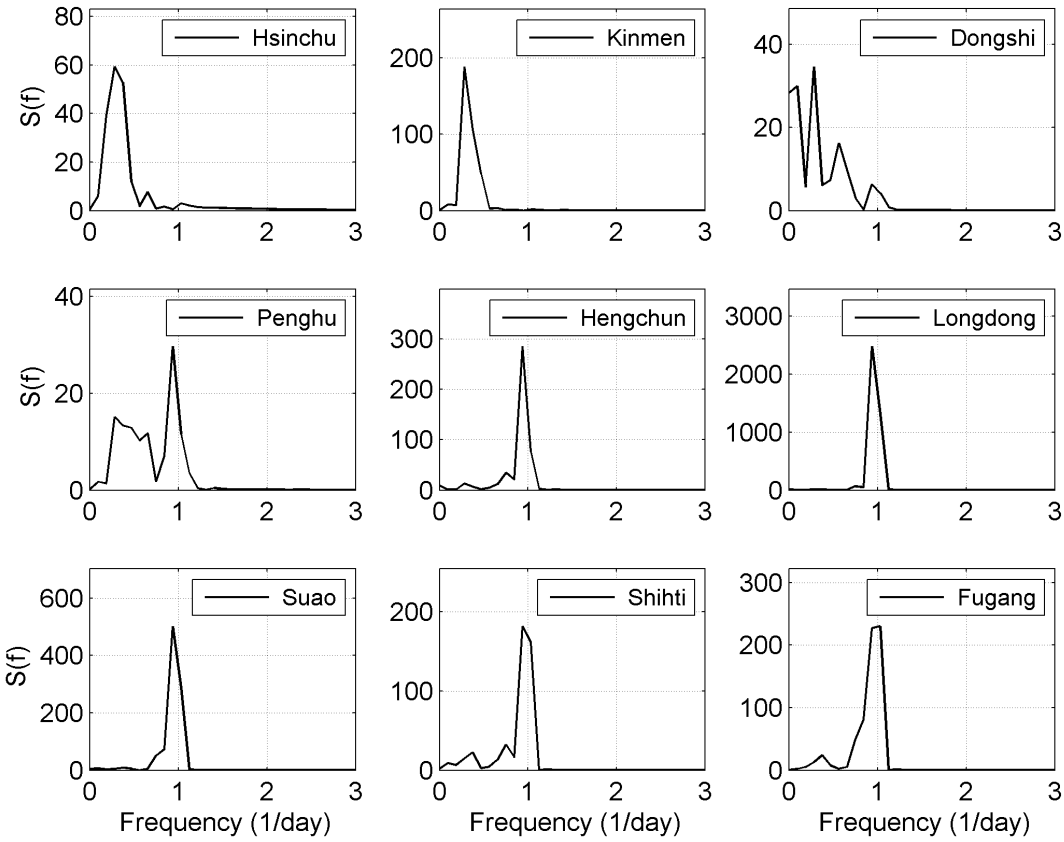

Fig. 19. Averaged spectra of IMF3 at different stations.

5. Conclusions

Synchronous high astronomical tide and storm surge have severe impact upon coasts and estuaries, resulting in possible flooding disaster in these areas. HA is a common and useful algorithm to separate tidal harmonics and nontidal residues, and storm surge magnitude is contained in nontidal residues. However, HA is recognized as a practical long-term data analysis. For short-term sea level data analysis, error from HA results would be unavoidable. The algorithm of EMD and EEMD was proposed for data and signal processing. Many studies have confirmed its practicability on nonlinear and nonstationary data processing. This study applies the EEMD to separate tidal harmonics and nontidal residues.

The analyzed results of EEMD present components of sea level data by different IMFs. By observing the orthogonality and completeness, this study reveals that the EEMD is applicable to decompose the sea level data. To describe the characteristics of tidal components, IMFs provide a different idea to monotonous amplitudes and periods of sinusoidal waves. For short-term sea level time series analysis, this work reveals that storm surge calculated results using EEMD are more accurate than

that using HA. Compared to EEMD results, calculated accuracy by the HA heavily relates to tidal range of the sea level area. The EEMD algorithm is practical for storm surge calculation for short-term analysis and high tidal range. However, two different residues from EEMD may be ideal to represent storm surge, making it necessary find out which one is best. This study proposes a way to determine the best residue using IMF spectra, which is verified by nine different tide stations around Taiwan, confirming it using more data sets from different stations around the world is necessary.

To understand the characteristics of storm surge calculation by EEMD, the current study calculates storm surge using various lengths of sea level records. Findings show that HA and EEMD should be complementary for storm surge calculation. HA is appropriate for long-term data analysis; the EEMD is predominant for short-term sea level data shorter than thirty-five days.

Acknowledgments

This work was supported by the Water Resources Agency (MOEAWRA0980270 and MOEAWRA0990248) and the National Science Council (98-2923-I-006-001-MY4) in Taiwan, R.O.C. The authors would like to offer their sincere thanks to the agencies. The support of the European Commission through FP7.2009-1, contract 244104 — THESEUS ("Innovative technologies for safer European coast in a changing climate"), is also gratefully acknowledged. In addition, the authors are grateful to the referees for helpful comments and suggestions.

References

Bode, L. & Hardy, T. A. [1997] "Progress and recent developments in storm surge modeling," *ASCE J. Hydraul. Eng.* **123**(4), 315–331.

Butler, A., Heffernan, J. E., Tawn, J. A., Flather, R. A. & Horsburgh, K. J. [2007] "Extreme value analysis of decadal variations in storm surge elevations," *J. Mar. Syst.* **67**, 189–200.

Chang, C. Y., Huang, N. E. & Shen, Z. [1997] "A statistically significance periodicity in the homestake solar neutrino data," *Chin. J. Phys.* **35**, 818–831.

Daetig, M. & Schlurmann, T. [2004] "Performance and limitations of the Hilbert–Huang transformation (HHT) with an application to irregular water waves," *Ocean Eng.* **31**, 1783–1834.

De Oliviera, M. M. F., Ebecken, N. F. F., De Oliviera, J. L. F. & De Azevedo Santos, I. [2009] "Neural network model to predict a storm surge," *J. Appl. Meteor. Climatol.* **48**(1), 143–155.

Eric Jones, J. & Marshall Davies, A. [2009] "Storm surge computations in estuarine and near-coastal regions: The Mersey estuary and Irish Sea area," *Ocean Dynamics* **59**, 1061–1076.

Gan, X., Huang, W., Yang, J. & Fu, B. [2008] "Internal wave packet characterization from SAR images using empirical mode decomposition (EMD)," *2008 Congress on Image and Signal Processing*, pp. 750–753.

Ho, C. R., Kuo, N. J. & Lin, C. Y. [2004] "Sea surface temperature trends in the waters adjacent to Taiwan from 1982 to 2003," *Proc. SPIE Int. Soc. Opt. Eng.*, pp. 220–227.

Huang, N. E., Shen, Z., Long, S. R., Wu, M. C., Shih, H. H., Zheng, Q., Yen, N. C., Tung, C. C. & Liu, H. H. [1998] "The empirical mode decomposition and the Hilbert spectrum for nonlinear and nonstationary time series analysis," *Proc. R. Soc. A* **454**, 903–995.

Kim, S. Y., Yasuda, T. & Mase, H. [2010] "Wave set-up in the storm surge along open coasts during Typhoon Anita original research article," *Coastal Eng.* **57**, 631–642.

Klionski, D. M., Oreshko, N. I., Geppener, V. V. & Vasiljeva, A. V. [2008] "Applications of empirical mode decomposition for processing nonstationary signals," *Pattern Recognit. Image Anal.* **18**(3), 390–399.

Lee, T. L. [2006] "Neural network prediction of a storm surge," *Ocean Eng.* **33**, 483–494.

McMahon, T. A., Vogel, R. M., Peel, M. C. & Pegram, G. G. S. [2007] "Global streamflows — Part 1: Characteristics of annual streamflows," *J. Hydrol.* **347**(3–4), 243–259.

Molla, M. K. I., Rahman, M. S., Sumi, A. & Banik, A. P. [2006] "Empirical mode decomposition analysis of climate changes with special reference to rainfall data," *Discrete Dyn. Nat. Soc.* **2006**, 1–17.

Moon, I. J., Kwon, J. I., Lee, J. C., Shim, J. S., Kang, S. K., Oh, I. S. & Kwon, S. J. [2009] "Effect of the surface wind stress parameterization on the storm surge modeling," *Ocean Modelling* **29**, 115–127.

Nunes, J. C., Bouaoune, Y., Delechelle, E., Niang, O. & Bunel, P. H. [2003] "Image analysis by bidimensional empirical mode decomposition," *Image and Vision Comput.* **21**, 1019–1026.

Peel, M. C., McMahon, T. A. & Pegram, G. G. S. [2009] "Assessing the performance of rational spline-based empirical mode decomposition using a global annual precipitation dataset," *Proc. R. Soc. A* **465**, 1919–1937.

Reeve, D., Chadwick, A. & Fleming, C. [2004] *Coastal Engineering*: *Processes, Theory and Design Practice* (Spon Press, New York).

Silvester, R. & Hsu, J. R. C. [1997] *Coastal Stabilization* (World Scientific, Singapore).

Vrijling, J. K. [2001] "Probabilistic design of water defense systems in the Netherlands," *Reliab. Eng. Syst. Saf.* **74**(3), 337–344.

Wu, Z. & Huang, N. E. [2008] "Ensemble empirical mode decomposition: A noise assisted data analysis method," *Adv. Adap. Data Anal.* **1**(1), 1–41.

Zhang, H. & Gai, Q. [2006] "Research on properties of empirical mode decomposition method," *Proc. 6th World Congress on Intelligent Control and Automation* (IEEE, Dalian, China), pp. 10001–10004.

Zhang, J., Yan, R. & Gao, R. X. [2009] "Ensemble empirical mode decomposition for machine health diagnosis," *Key Eng. Mater.* **413–414**, 167–174.